

**SAGE-Spectroscopy:**  
The life-cycle of dust and gas in the  
Large Magellanic Cloud  
(PI: F. Kemper, PID: 40159)

Data delivery document v3.0

Paul M. Woods, G.C. Sloan, Karl D. Gordon, B. Shiao, F. Kemper,  
R. Indebetouw & the SAGE-Spec team

Spring 2011

# Contents

<b>1</b>	<b>Overview</b>	<b>3</b>
1.1	Introduction to SAGE-Spec . . . . .	3
1.2	Current data release . . . . .	4
1.3	Previous data releases . . . . .	4
1.3.1	Delivery 2 . . . . .	4
1.3.2	Delivery 1 . . . . .	5
1.4	Future data releases; timeline . . . . .	5
1.5	Database format . . . . .	8
1.5.1	IRS staring point source data . . . . .	8
1.5.2	MIPS-SED point source data . . . . .	10
1.5.3	IRS & MIPS-SED extended region data . . . . .	10
1.6	Format of plots . . . . .	11
1.7	Photometric matching of point source data . . . . .	11
1.8	Core team members . . . . .	12
1.9	Extended team members . . . . .	13
1.10	Contact information . . . . .	13
1.11	Acknowledgments . . . . .	13
<b>2</b>	<b>IRS spectroscopy</b>	<b>14</b>
2.1	Point sources . . . . .	14
2.1.1	Observation settings . . . . .	14
2.1.2	Data processing . . . . .	14
2.1.3	Low-resolution spectra . . . . .	15
2.1.4	High-resolution spectra . . . . .	17
2.1.5	Quality control of the data . . . . .	18
2.1.6	Caveats . . . . .	18
2.1.7	Point source classification . . . . .	19
2.2	Extended sources . . . . .	19
2.2.1	Observation settings . . . . .	20
2.2.2	Data processing . . . . .	20
2.2.3	Quality control of the data . . . . .	21

---

<b>3</b>	<b>MIPS-SED spectroscopy</b>	<b>23</b>
3.1	Point sources . . . . .	23
3.1.1	Observation settings . . . . .	23
3.1.2	Data processing . . . . .	23
3.1.3	Quality control of the data . . . . .	24
3.2	Extended sources . . . . .	24
3.2.1	Observation settings . . . . .	24
3.2.2	Data processing . . . . .	24
3.2.3	Quality control of the data . . . . .	24
<b>A</b>	<b>Availability of spectra and photometry</b>	<b>27</b>
<b>B</b>	<b>Quality control results for IRS spectra</b>	<b>33</b>
	<b>References</b>	<b>39</b>

# Chapter 1

## SAGE-Spec overview

### 1.1 Introduction to the goals of the SAGE-Spec program

The SAGE-Spectroscopy legacy proposal (SAGE-Spec; PI: F. Kemper, PID: 40159; Kemper et al. 2010) is the spectroscopic follow-up to the successful SAGE-LMC legacy program (Meixner et al. 2006; PI: M. Meixner, PID: 20203) that mapped the Large Magellanic Cloud (LMC) with all bands of the IRAC and MIPS instruments on board the Spitzer Space Telescope. The acronym SAGE stands for Surveying the Agents of Galaxy Evolution, and thus the project aims to make an inventory of the budget of gas and dust involved in the life-cycle of matter in the Magellanic Clouds.

The SAGE-Spec legacy program has used the IRS and the SED mode on the MIPS instrument to obtain spectroscopic information of a representative sample of point sources and extended regions in the LMC, with two goals in mind:

The first goal is to study the composition and properties of gas and dust in environments relevant to the life-cycle of matter, from evolved stars to the interstellar medium and ultimately to star-forming regions. Combining this information with statistics obtained from the SAGE-LMC project will allow us to get a complete picture of the cycle of gas and dust in terms of mass *and* in terms of composition and physical properties.

Secondly, sources in the SAGE-LMC point source catalogue will be classified using a classification scheme tested against the SAGE-Spec sample. In addition to the observations made within the context of the SAGE-Spec proposal, we have extended the sample to contain *all* IRS and MIPS-SED observations within the original SAGE-LMC footprint (“the archival sample”).

In total, 224.6 hours of observations were made and 196 positions were targeted with the IRS instrument, resulting in 197 point sources being observed; 48 point sources were observed with MIPS in SED mode and 20 extended regions were also targeted with MIPS: 10 HII regions and 10 diffuse regions. In addition, the reduction and delivery of all the IRS and MIPS-SED spectroscopic data within the SAGE-LMC footprint adds a further  $\sim 900$  IRS (mostly point-source) targets and several other extended regions. See Kemper et al. (2010) for an overview of the project.

Of the 196 point sources observed with IRS, all were observed using the Short-Low module (SL;  $\lambda \approx 5\text{--}14 \mu\text{m}$ ), and 128 were also observed using Long-Low (LL;  $\lambda \approx 14\text{--}37 \mu\text{m}$ ). Upon ex-

amination, the LL observation of one source, SSID16 (GV 60), picked up another target rather than the intended target. Thus there are 197 distinct point sources in the proposal sample at this point. Spectra of a number of serendipitous objects were obtained, and these will be delivered in a future data release. 48 of the brightest points sources were also targeted with MIPS in SED mode and a number of serendipitous sources were also found, bringing the total of MIPS-SED point sources up to 63. For our source selection strategy, please see the overview publication for the project, Kemper et al. (2010).

## 1.2 Description of the observations in the current data release

The final SAGE-Spec delivery contains all the reduced IRS staring data from the Spitzer archive within the SAGE footprint (Table 1.1), totalling 883 spectra. This includes calibration data. This marks a complete delivery of IRS staring data from in-orbit checkout through to the end of Cycle 5. We also include higher-level products: integrated spectra for all IRS and MIPS-SED extended region data, and the object classification for the original 197 SAGE-Spec IRS point sources, as discussed in Woods et al. (2011).

This delivery also includes several updates. Previously-delivered IRS staring data from the SAGE-Spec program have been updated to the S18.18 standard. We also deliver revised reduced data of IRS and MIPS-SED extended regions, accounting for the recently-identified “dark settle” problem (see §2.2.3).

As a bonus, we also include various reduced IRS staring spectra from the programs found in Table 1.1 which fall outside of the SAGE footprint. These have SSIDs of 5000+, and do not form part of the official SAGE-Spec delivery.

## 1.3 Description of the observations in previous data releases

### 1.3.1 Delivery 2

The second delivery of data from the SAGE-Spec Spitzer Legacy Program improved upon the data delivered in delivery #1 and added both IRS and MIPS-SED data on point sources and extended regions observed in the LMC with Spitzer. We delivered reduced data from the Spitzer archive that falls within the SAGE footprint on the LMC. This delivery included IRS staring mode data from Spitzer cycles 1–3 and the Guaranteed Time Observations (GTOs). It comprised 403 spectra of 352 objects or lines of sight. Details of program data included can be found in Table 1.1. We matched these spectral data with near- and mid-IR photometry (see below). In addition, we updated some of the matching broadband photometry previously delivered with the 197 SAGE-Spec proposal point sources.

We also released IRS mapping data of 23 diffuse and HII regions in the form of order cubes, 3 of which were taken from the Spitzer archive. All but one (SSDR12) of these regions are also covered by MIPS-SED observations, for which we also delivered reduced data. Our previous reductions of MIPS-SED data of 48 point sources were revised, and several serendipitous sources were added to the sample so that the number now totals 61 (with 63 spectra; Table 1.2).

### 1.3.2 Delivery 1

In the first delivery of SAGE-Spec data in August 2009 we delivered IRS staring mode spectra of 197 point sources and MIPS-SED spectra of 48 point sources selected from the SAGE catalogue. The IRS staring mode spectra are complemented by matching photometry from SAGE (IRAC and MIPS; Meixner et al. 2006), MCPS (Zaritsky et al. 2004), 2MASS (Skrutskie et al. 2006) and IRSF (Kato et al. 2007). We also delivered Postscript plots of the 197 the IRS spectra with associated photometry.

## 1.4 Description of the observations in future data releases and delivery timeline

Further data releases from the SAGE-Spec project will include:

- Object classifications for the entire Spitzer IRS archive located within the SAGE footprint (GTO, cycles 1–5, calibration data).
- Spectral classifications for the entire Spitzer IRS archive located within the SAGE footprint (GTO, cycles 1–5, calibration data).
- Statistical object classification of the SAGE point source catalogue.
- Feature maps of extended regions covered by IRS and MIPS-SED observations.

Minor update deliveries may be made for revised data reductions. Due to the closure of the Spitzer Science Centre, these deliveries will be made to IRSA directly, and/or presented in journal articles.

Table 1.1: Archival IRS staring data in the present delivery

Cycle	Program ID	Program PI	notes
Calsfx	M – 28	Various	14 hires, 43 lores spectra
1 (GTO)	18	Uchida	10 hires spectra
1 (GTO)	63	Brandl	19 hires, 17 lores spectra
1 (GTO)	103	Bernard-Salas	18 hires, 18 lores spectra
1 (GTO)	124, 129	Gehrz	6 slhi, 2 lores spectra
1 (GTO)	200	Sloan	29 lores spectra
1 (GTO)	249	Indebetouw	6 lores spectra
1 (GTO)	263	Woodward	1 lores spectrum
1 (GTO)	464, 472	Cohen	14 lores spectra
1 (GTO)	485	Ardila	6 lores spectra
1	1094	Kemper	9 hires, 2 slhi, 9 lores spectra
1	2333	Woodward	4 slhi spectra
1	3426	Kastner	60 lores spectra

continued on next page...

Table 1.1 – continued from previous page

Cycle	Program ID	Program PI	notes
1	3470	Bouwman	1 hires spectrum
1	3483	Rho	1 lores spectrum
1	3505	Wood	31 lores spectra
1	3578	Misselt	13 lores spectra
1	3583	Onaka	12 lores spectra
1	3591	Kemper	53 lores spectra
2	20080	Polomski	1 lores spectrum
2	20443	Stanghellini	20 lores spectra
2	20752	Reynolds	1 hires spectrum
3	30067	Dwek	4 lores spectra
3	30077	Evans	1 lores spectrum
3	30180	IRAC	1 lores spectrum
3	30332	Sloan	1 lores spectrum
3	30345	Sloan	4 hires spectra
3	30372	Tappe	7 lores spectra
3	30380	Clayton	1 lores spectrum
3	30544	Morris	1 lores spectrum
3	30788	Sahai	24 lores spectra
3	30869	Kastner	1 slhi, 8 lores spectra
4	40031	IRAC	2 lores spectra
4	40149	Dwek	4 lores spectra
4	40604	Reynolds	2 lores spectra
4	40650	Looney	8 hires, 331 slhi spectra
5	50092	Gielen	10 lores spectra
5	50147	Sloan	6 hires spectra
5	50167	Clayton	7 lores spectra
5	50338	Matsuura	11 hires, 1 slhi, 23 lores spectra
5	50444	Dwek	3 hires, 2 lores spectra

Table 1.2: Point sources observed in MIPS-SED mode

SSID	Source name	Co-ordinates (J2000)	AOR key	Deliv.#2 SSID
600	SAGE1C J043727.60-675435.0	4h37m27.61s, -67d54m35.0s	22459648	500
601	SMP-LMC-11	4h51m37.82s, -67d05m17.0s	22450432	501
602	IRAS04530-6916	4h52m45.70s, -69d11m49.4s	22453504	502
603	IRAS04537-6922	4h53m30.11s, -69d17m49.3s	22457088	503
604	LH $\alpha$ 120-N89	4h55m06.53s, -69d17m08.5s	22460416	504
605	WOH 6064	4h55m10.48s, -68d20m29.9s	22448640	505
606	IRAS04557-6639	4h55m50.59s, -66d34m34.7s	22457344	506
607	IRAS04562-6641	4h56m22.59s, -66d36m56.8s	22457600	507

continued on next page...

Table 1.2 – continued from previous page

SSID	Source name	Co-ordinates (J2000)	AOR key	Former SSID
608	R66	4h56m47.08s, -69d50m24.8s	22453760	508
609	R71	5h02m07.40s, -71d20m13.0s	22454016	509
610	IRAS05047-6644	5h04m47.00s, -66d40m30.3s	22451456	510
611	SMP-LMC-21	5h04m51.97s, -68d39m09.5s	22450688	511
612	SMP-LMC-28	5h07m57.62s, -68d51m47.3s	22450944	512
613	SMP-LMC-36	5h10m39.60s, -68d36m04.9s	22459664	513
614	IRAS05137-6914	5h13m24.66s, -69d10m48.1s	22452992	514
615	MSX-LMC222	5h13m41.99s, -69d35m26.7s	22451712	515
616	SAGE1C J051347.73-693505.3	5h13m46.5s, -69d35m10s	22451712	—
617	MSX-LMC349	5h17m26.93s, -68d54m58.7s	22449920	516
618	IRAS05216-6753	5h21m29.68s, -67d51m06.6s	22451968	517
619	SAGE1C J052222.95-684101.0	5h22m22.96s, -68d41m01.1s	22457856	518
620	HS270-IR1	5h23m53.93s, -71d34m43.8s	22458112	519
621	SMP-LMC-62	5h24m55.08s, -71d32m56.1s	22451200	520
622	LH $\alpha$ 120-N51-YSO1	5h26m01.22s, -67d30m11.9s	22458368	521
623	LH $\alpha$ 120-N49	5h26m03.10s, -66d05m17.2s	22454272	522
624	LH $\alpha$ 120-N49	5h26m07s, -66d05m00s	22454272	—
625	MSX-LMC577	5h26m30.60s, -67d40m36.7s	22455296	523
626	LH55	5h26m38.6s, -67d39m23s	22455296	—
627	IRAS05281-7126	5h27m23.14s, -71d24m26.3s	22458624	524
628	IRAS05280-6910	5h27m40.06s, -69d08m04.6s	22454528	525
629	IRAS05291-6700	5h29m07.59s, -66d58m15.1s	22450176	526
630	IRAS05298-6957	5h29m24.53s, -69d55m15.9s	22448896	527
631	IRAS05325-6629	5h32m31.95s, -66d27m15.2s	22452224	528
632	IRAS05328-6827	5h32m38.59s, -68d25m22.4s	22452480	529
633	RP775	5h32m44.40s, -69d30m05.5s	22459904	530
634	IRAS05330-6826	5h32m48.3s, -68d23m59s	22452480	—
635	SAGE1C J053249.35-693036.8	5h32m49.4s, -69d30m37s	22459904	—
636	IRAS05329-6708	5h32m51.36s, -67d06m51.8s	22449152	531
637	MSX-LMC783	5h32m55.44s, -69d20m26.6s	22455552	532
638	HV2671	5h33m48.92s, -70d13m23.6s	22454784	533
639	SN 1987A	5h35m23.8s, -69d17m07s	17720320	—
640	MSX-LMC741	5h35m25.83s, -71d19m56.6s	22455808	534
641	SN 1987A	5h35m31.5s, -69d17m09s	22393344	—
642	SN 1987A	5h35m38.1s, -69d16m43s	17721600	—
643	SN 1987A	5h35m38.2s, -69d16m43s	22394624	—
644	R126	5h36m25.85s, -69d22m55.7s	22455040	535
645	30Dor-17	5h37m28.09s, -69d08m47.8s	22452736	536
646	H88b 86?	5h38m40.9s, -69d25m14s	22460672	—
647	LH $\alpha$ 120-N158B	5h38m44.53s, -69d24m38.3s	22460672	537

continued on next page...



Table 1.2 – continued from previous page

SSID	Source name	Co-ordinates (J2000)	AOR key	Former SSID
648	LH $\alpha$ 120-N159-P2	5h39m41.86s, -69d46m11.9s	22453248	538
649	LH $\alpha$ 120-N159-K4?	5h39m55.0s, -69d46m16s	22459136	—
650	LH $\alpha$ 120-N160-1	5h39m59.49s, -69d37m30.3s	22458880	539
651	LH $\alpha$ 120-N159S	5h40m00.67s, -69d47m13.4s	22459136	540
652	LH $\alpha$ 120-N160-3	5h40m04.4s, -69d38m21s	22458880	—
653	UFO1	5h40m11.83s, -70d10m04.2s	22456064	541
654	WOH-G457?	5h40m11.95s, -70d09m15.7s	22449408	542
655	RP85	5h40m33.57s, -70d32m40.3s	22460160	543
656	SAGE1C J054043.15-701110.3	5h40m43.18s, -70d11m10.3s	22456320	544
656	SAGE1C J054043.15-701110.3	5h40m43.18s, -70d11m10.3s	22456832	—
657	MSX-LMC1794	5h40m44.00s, -69d25m54.5s	22456576	545
658	MSX-LMC956	5h40m49.27s, -70d10m13.6s	22456832	546
658	MSX-LMC956	5h40m49.27s, -70d10m13.6s	22456320	—
659	BSDL2955	5h45m43.9s, -67d09m55s	22459392	—
660	BSDL2959	5h45m44.80s, -67d09m28.2s	22459392	547

Table 1.2: The reader is also referred to van Loon et al. (2010) for integration times, quality control and other information.

## 1.5 Format of the database at the Spitzer Science Center

The SAGE-Spec database can be reached via the Legacy page on the Spitzer Science Center website, or via direct links:

<http://irsa.ipac.caltech.edu/data/SPITZER/SAGE/>

<http://ssc.spitzer.caltech.edu/legacy/sagespechistory.html>

The database is made up of a tables of metadata and associated data products (FITS files, FITS data cubes, plots of spectra and associated photometry). The format of these tables is slightly different for the IRS staring data and the MIPS-SED data.

### 1.5.1 IRS staring point source data

The IRS staring spectra have an associated metadata file, which is in IPAC tbl format. This table has slightly different formats for the SAGE-Spec proposal targets (delivered to the SSC in August 2009) and the Spitzer archival targets (first delivered to the SSC in February 2010).

**SAGESpecID:** This is a unique identifier for each target. SAGE-Spec point sources are labelled with numbers 1–197, which are obtained by ordering the sources sequentially according to Right Ascension (R.A.). Archival sources in this delivery are labelled 4000–4817.

**label:** This is a unique identifier for each spectrum. It is constructed by concatenating R.A. (to 4 decimal places) and declination (dec; to 4 decimal places), instrument name (i.e., IRSX or MIPS) and module name with nod or processing information, for example: 79.7943-69.5629\_IRSX\_SL\_(scaled).

For the archival targets, this label also includes the SAGE-Spec ID and an integer which increments with every associated spectrum, for example:

70.1187-69.9202\_IRSX\_1006\_1\_SL\_LL\_(scaled)

70.1190-69.9203\_IRSX\_1006\_2\_SH\_LH\_(scaled)

70.1192-69.9206\_IRSX\_1006\_3\_LL\_(scaled)

For further details, see **modules**, below).

**ra**: Right ascension Field-Of-View (FOV) co-ordinates (J2000)<sup>1</sup>.

**dec**: Declination FOV co-ordinates (J2000)<sup>1</sup>.

**SAGEIRACID**: Associated SAGE-LMC IRAC source designation.

**SAGEMIPSID**: Associated SAGE-LMC MIPS 24  $\mu\text{m}$  source designation.

**AORkey**: Astronomical Observation Request (AOR) number of the Spitzer observation.

**progid**: Program ID in which data were obtained (for SAGE-Spec this is 40159).

**instrument**: IRSX for Infrared Spectrograph, MIPS for Multiband Imaging Photometer for Spitzer.

**modules**: One of:

SL, LL (scaled)

SL, LL (unscaled)

SL (scaled)

SL (unscaled)

LL (scaled)

LL (unscaled)

SL Order 1 Nod 1

SL Order 1 Nod 2

SL Order 2 Nod 1 plus bonus order

SL Order 2 Nod 2 plus bonus order

LL Order 1 Nod 1

LL Order 1 Nod 2

LL Order 2 Nod 2 plus bonus order

LL Order 2 Nod 1 plus bonus order

---

<sup>1</sup>We purposefully choose to use FOV co-ordinates (i.e., `ra_fov` and `dec_fov` in the FITS headers) over requested co-ordinates (`ra_rqst` and `dec_rqst`, also found in FITS headers, and which are those obtained when one queries via Leopard, for example) since the FOV co-ordinates most accurately determine the region of space the telescope is pointing at. In general, FOV co-ordinates differ from requested co-ordinates by  $\approx 0''.75$ . However, in extreme cases, there can be a difference of up to  $\approx 5''.7$  between the two co-ordinate systems in the SAGE-Spec IRS sample.

SH, LH (scaled) [archival data only]

SH, LH (unscaled) [archival data only]

SL, SH (scaled) [archival data only]

SL, SH (unscaled) [archival data only]

In most cases, the end user will require just the SL, LL (scaled) version of the spectrum or equivalent high-resolution spectrum.

**pipelineVersion:** Spitzer data reduction pipeline version.

**objectName:** Chosen name for object, usually the oldest historically.

**alternateName:** Other useful identifiers.

**quality:** Data quality notes are: 'OK'; 'Wa' (warning, use spectrum with caution); 'Fa' (fatal, spectrum is bad) – see the notes field for an explanation [archival data only]

**notes:** quality control comments detailing any data complexities [archival data only]

Spectra are then available separately as single files or a large archive, with or without additional photometry points. Please see the README file for further information.

### 1.5.2 MIPS-SED point source data

The MIPS-SED data are available as separate files with incorporated metadata. Column headings are:

**SAGESpecID:** This is a unique identifier for each point source. MIPS-SED sources are labelled with numbers 500–562, which are obtained by ordering the sources sequentially according to Right Ascension (R.A.).

**label:** This is a unique identifier for each spectrum. It is constructed by concatenating R.A. (to 4 decimal places) and declination (dec; to 4 decimal places), instrument name (MIPSSSED) and an optional integer increment for sources with more than one spectrum, for example: 85.1799-70.1862\_MIPSSSED.2.

**ra:** Right ascension co-ordinates (J2000)

**dec:** Declination co-ordinates (J2000)

**objectName:** Chosen name for object.

**quality:** This can be one of "good", "ok", "poor" and "bad". These terms are explained in Section 3.1.3.

**waveLength:** wavelength in microns.

**flux:** flux in Jansky units.

**fluxUnc:** flux uncertainty in Jansky units.

**SN:** signal-to-noise ratio.

**sky:** sky noise.

### 1.5.3 IRS & MIPS-SED extended region data

Metadata for extended region data comprises of:

**Name:** Chosen name for object; SDR represents SAGE-Spec Diffuse Region, DEM numbers are taken from the catalogue of Davies et al. (1976).

**ra:** Right ascension co-ordinates (J2000)

**dec:** Declination co-ordinates (J2000)

**IRS SL AORID:** AOR number for IRS SL observation.

**IRS LL AORID:** AOR number for IRS LL observation.

**MIPS-SED AORID:** AOR number for MIPS-SED observation.

This data is also presented in Table 2.1.

## 1.6 Format of the plots which accompany the data delivery

Each plot, which has a filename of `<label>.ps` (e.g., `76.2155-66.6354_IRSX_SL_LL_scaled.ps`), is composed of four panels (see Fig. 1.1). Clockwise from the top-left these panels represent:

Full IRS spectrum plotted with error bars.

Full IRS spectrum plotted with modules in different colours to show where the joins lie.

Spectral energy distribution with photometric points and IRS spectrum, shown in log scale.

Spectral energy distribution with photometric points and IRS spectrum, shown in linear scale.

Each plot also includes the SAGE-Spec ID and the chosen point source name.

## 1.7 Photometric matching of point source data

For each SAGE-Spec and archival source a cone search using a radius of  $20''$  is performed against the SAGE-LMC photometric database. The possible matches are retained in the following manner:

1. Only the closest match in each of the categories below are chosen.
2. Each of these closest matches is further restricted:
  - (a) IRAC (3.6, 4.5, 5.8, 8.0  $\mu\text{m}$ ) matches must be within  $3''$ .
  - (b) MIPS  $24\mu\text{m}$  matches must be within  $3''$ .
  - (c) MIPS  $70\mu\text{m}$  matches must be within  $10''$ .
  - (d) MIPS  $160\mu\text{m}$  matches must be within  $20''$ .
  - (e) Two Micron All Sky Survey (2MASS) JHK matches must be within  $3''$ .
  - (f) Infrared Survey Facility (IRSF) JHK matches must be within  $3''$ .
  - (g) Magellanic Clouds Photometric Survey (MCPS) UVBI matches must be within  $3''$ .

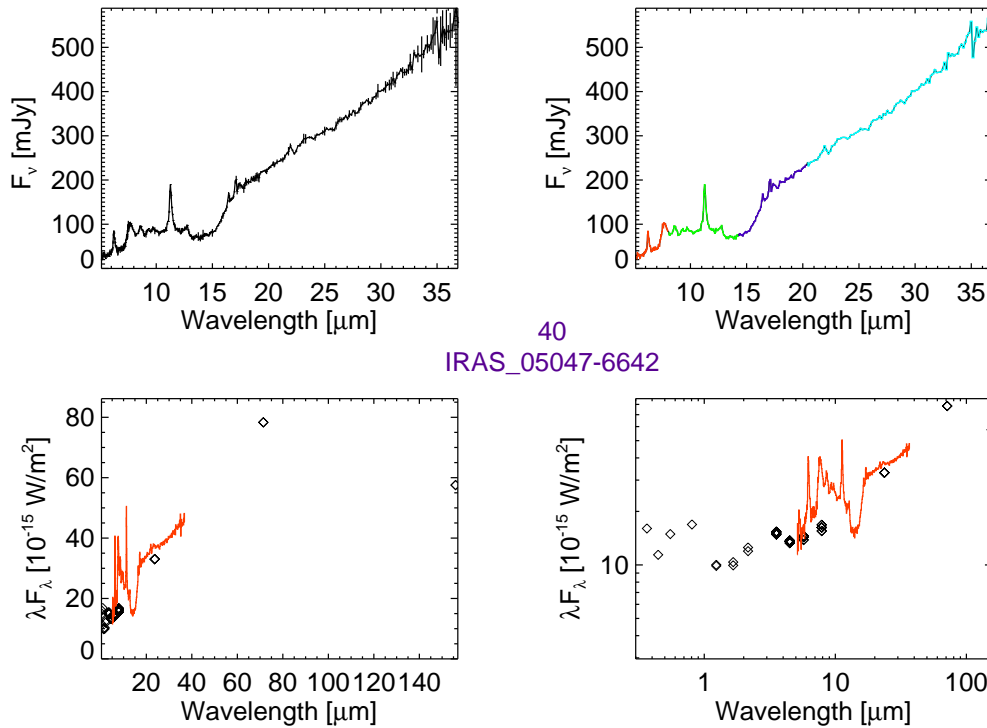


Figure 1.1: An example plot of the IRS staring data for SAGE-Spec source 40 (see text).

## 1.8 Core team members

**Ciska Kemper (Academia Sinica, Institute of Astronomy and Astrophysics/University of Manchester):** PI, science overview, observing strategy.

**Karl Gordon (Space Telescope Science Institute):** IRS extended region and MIPS-SED data reduction.

**Margaret Meixner (Space Telescope Science Institute):** science overview, observing strategy, database, SAGE-LMC photometry liaison.

**Remy Indebetouw (University of Virginia/NRAO):** quality control, IRS extended region data reduction.

**Massimo Marengo (Iowa State University):** source classification.

**Greg Sloan (Cornell University):** IRS staring data reduction, observing strategy.

**Xander Tielens (Leiden Observatory):** science overview.

**Jacco van Loon (Keele University):** observing strategy, quality control.

**Paul Woods (University College London/University of Manchester):** Project Manager, quality control, source classification.

## 1.9 Extended team members

V. Antoniou (Iowa), J.-P. Bernard (CESR, Toulouse), R. D. Blum (NOAO), M. L. Boyer (STScI), C.-H. R. Chen (U. Virginia), M. Cohen (Berkeley), C. Dijkstra, M. Galametz (CEA, Saclay), F. Galliano (CEA, Saclay), C. Gielen (KU Leuven), V. Gorjian (JPL/Caltech), J. Harris (Steward Observatory), H. Hirashita (ASIAA), S. Hony (CEA, Saclay), J. Hora (Harvard CfA), R. Indebetouw (U. Virginia/NRAO), O. Jones (U. Manchester), A. Kawamura (Nagoya University), K. E. Kraemer (AFRL), E. Lagadec (ESO), K.-H. Law (JHU), B. Lawton (STScI), J. Leisenring (U. Virginia), S. Madden (CEA, Saclay), M. Matsuura (UCL), I. McDonald (U. Manchester), C. McGuire (U. Manchester), B. O'Halloran (Imperial College London), K. Olsen (NOAO), J. Oliveira (Keele), M. Otsuka (STScI), R. Paladini (SSC), D. Paradis (SSC), W. T. Reach (SSC), D. Riebel (StScI), D. Rubin (CEA, Saclay), K. Sandstrom (MPIA), B. Sargent (STScI), J. Seale (STScI), M. Sewiło (STScI), B. Shiao (STScI), A. K. Speck (U. Missouri), S. Srinivasan (IAP), R. Szczerba (N. Copernicus Astronomical Center. Toruń), A. G. G. M. Tielens (Leiden Observatory), E. van Aarle (KU Leuven), J. van Benthem (Cornell), S. D. Van Dyk (SSC), H. Van Winckel (KU Leuven), U. Vijh (U. Toledo), K. Volk (STScI), B. Whitney (Space Science Institute, Boulder), A. Wilkins (Cornell), M. Wolfire (U. Maryland), R. Wu (CEA, Saclay), A. Zijlstra (U. Manchester).

## 1.10 Contact information

**General questions:** Ciska Kemper (ciskakemper@fastmail.net), Paul Woods (pmw@star.ucl.ac.uk)

**MIPS-SED extended data:** Karl Gordon (kgordon@stsci.edu)

**IRS extended region data:** Karl Gordon (kgordon@stsci.edu), Remy Indebetouw (remy@virginia.edu)

**MIPS-SED point sources:** Jacco van Loon (jacco@astro.keele.ac.uk)

**IRS staring data:** Greg Sloan (sloan@isc.astro.cornell.edu), Paul Woods (pmw@star.ucl.ac.uk)

**Database questions:** Bernie Shiao (shiao@stsci.edu), Margaret Meixner (meixner@stsci.edu)

## 1.11 Acknowledgments

This publication makes use of data products from the Two Micron All Sky Survey (2MASS), which is a joint project of the University of Massachusetts and the Infrared Processing and Analysis Center/California Institute of Technology, funded by the National Aeronautics and Space Administration and the National Science Foundation.

MCPS data are publicly available from

<http://ngala.as.arizona.edu/dennis/mcsurvey.html>

The IRSF website is at: [http://www.z.phys.nagoya-u.ac.jp/~irsf/index\\_e.html](http://www.z.phys.nagoya-u.ac.jp/~irsf/index_e.html)

## Chapter 2

# IRS spectroscopy

### 2.1 Point sources

#### 2.1.1 Observation settings

All IRS observations of point sources in this data delivery were obtained in staring mode. The majority used SL, usually in combination with LL, and we have delivered these data as full low-resolution spectra (lores; 5–37 $\mu\text{m}$ ). A minority used the Short-High (SH) module, usually with Long-High (LH), and we have delivered these where possible as full high-resolution spectra (hires; 10–37 $\mu\text{m}$ ). Some observers used a combination of SL, SH and LH; we have delivered these data in a SL-hires combination (slhi).

Each target in the SAGE-Spec program was observed after a high-accuracy peak-up, usually on the target itself. In cases where the target was too bright or faint or in a crowded region, the telescope peaked up on a nearby 2MASS source. Most of the spectra observed in other programs also used a similar strategy, but some used moderate-accuracy peak-up, blind peak-up, or the PCRS camera on Spitzer.

In the SAGE-Spec program, observations were designed so that the number and length of integration cycles matched for the two apertures matched in low-resolution modules, in order to maximize the options for background subtraction. Most of the larger programs designed by other users followed a similar course, but not all. The user of these data should keep in mind that with the large number of different astronomers designing observations, virtually any combination of apertures, integration times, and number of cycles is possible. As an example, one program observed using only the SL order-1 aperture.

All SAGE-Spec IRS staring data were obtained by the Spitzer Space Telescope from IRS Campaigns 47 to 53. These covered the period from January 9 to August 16 2008. The SAGE-Spec data delivery includes IRS observations obtained by other programs beginning with in-orbit checkout (IOC) and continuing all the way through Cycle 5.

#### 2.1.2 Data processing

The IRS data in this delivery were processed using the SSC pipeline S18.18. Before spectra were extracted, the background was subtracted from each image, and the resulting difference image

was cleaned to replace pixels flagged as bad with data from neighbouring pixels. Spectra were extracted from individual images, then calibrated and co-added.

### 2.1.3 Low-resolution spectra

For SL, the default background subtraction was an aperture difference, where an image with the source in one aperture served as the background for the image with the source in the other aperture, but the same nod position. For example, for SL1 nod 1, the background image was SL2 nod 1. For LL, the default was a nod difference, where the image with the source in one nod position served as the background for the image with the source in the other nod position in same aperture. Thus LL1 nods 1 and 2 served as backgrounds for each other, and likewise for LL2 nods 1 and 2.

In many cases, complex backgrounds or additional sources in the on-target aperture or off-target aperture forced us to modify the background subtraction. In addition to aperture or nod differences, we occasionally resorted to cross differences (other aperture, other nod). In some cases, no suitable background subtraction was possible, which could result in compromised or useless spectroscopy. See Section 2.1.5 for more detailed information.

We relied on the `bmask` images supplied with each data image by the SSC and the campaign rogue masked produced by the SSC to identify bad pixels. Any pixel with a `bmask` value of 4096 or higher was replaced. Any pixel which was identified as a rogue in any two campaigns from the start of the mission through Camp. 54 was also replaced. Additionally, all NaNs in the data were replaced.

To replace bad pixels, we applied the `imclean.pro` IDL procedure written at Cornell University. This algorithm now serves as the core of the pixel-replacement within `irsclean.pro`, which is provided by the SSC. To replace a bad pixel, the spatial profile of neighbouring rows are scaled to the row with the bad pixel. A replacement value is constructed from good data in the same column. This algorithm assumes that spatial structure of the source is unchanged over the rows in question and thus it could break down in the vicinity of spectral changes in spatial structure, such as spatially extended emission from a forbidden line near an unresolved continuum source.

To extract spectra from the spectral images, we used the `profile`, `ridge`, and `extract` modules of the SSC pipeline. These are available within SPICE. The resulting extraction is equivalent to a tapered-column extraction within SMART, with the extraction aperture two pixels wide in the dispersion direction and increasing in width in the cross-dispersion (spatial) direction linearly with wavelength. The extraction apertures are defined as follows:

order	width (pix)	wavelength ( $\mu\text{m}$ )
SL2	4.000	6.0
SL-bonus	5.333	8.0
SL1	8.000	12.0
LL2	4.250	16.0
LL-bonus	5.445	20.5
LL1	7.172	27.0

Spectra are extracted from each spectral image in a given nod position, then calibrated from



digital units to flux density units (Janskys). The spectral correction is based on comparison of similarly processed spectra of calibration stars to spectral templates for those stars produced at Cornell. HR 6348 (K0 III) served as the calibrator for all SL data. It and the K5 giant HD 173511 (K5 III) served as the calibrators for all LL data.

The “truth” spectra of these standards were constructed using ratios to low-resolution IRS spectra of the A1 dwarfs  $\alpha$  Lac and  $\delta$  UMi, using a generic Kurucz model of an A1 dwarf as the starting “truth” spectrum. This new calibration differs from previous deliveries because we have dropped our assumed photometric levels by 5% to bring them into line with the current 24- $\mu$ m MIPS calibration (Engelbracht et al. 2007; Rieke et al. 2008). A paper describing this process in more detail is in preparation (Sloan et al. 2011).

The spectrum reported for each nod position includes the mean of the individually extracted spectra in that position, and the formal uncertainty in the mean (standard deviation / square root of the number of images). The individual nod spectra are included in this data delivery.

To produce a complete spectrum for SL and LL, which are also included in this delivery, we average the spectra from the two nods, and we append the data from the three orders to each other. When combining the nods, spikes and divots which appear in only one nod but not the other are rejected. In these cases, only the data from the better-behaved nod are used. New uncertainties in the mean are calculated (before spike rejection, not after), and if they are larger than the propagated error from the two nods, are used in their place. Note that the formal uncertainty in the mean of two data is just half the difference in the data.

Thus this data delivery includes five spectra from SL and five from LL (the combined spectrum from the module and the four components from both nods in both apertures). In addition, we also provide a combined low-resolution spectrum, produced by appending the LL data to the SL, and a final low-resolution spectrum, corrected for discontinuities between segments (stitched), and with extraneous data removed (trimmed).

To produce this final spectrum, we assume that the discontinuities between spectral segments arise from pointing errors, which lead to partial truncation of mispointed sources by the slit edges. Thus, segments are calibrated upwards to the presumably best-centered segment. This usually means that SL is scaled upward to LL, since pointing errors have more impact in the smaller SL slit. The corrections are multiplicative scalar corrections and have no dependence on wavelength. This assumption is reasonable for corrections of roughly 10% or less. For larger corrections, the general shape of the continuum can no longer be relied upon as accurate. The bonus-order data have been combined with overlapping first- and second-order data before spectra are corrected for discontinuities. The corrections are calculated using the wavelengths of overlap between adjacent spectral segments. In the case of SL2 and LL2, the bonus order which were taken at the same time, and with the target at the same place in the aperture, provide the overlap needed between first- and second-order data.

Two more modifications have been made to spectra in the final delivered product. Any uncertainty which suggests a signal/noise ratio greater than 500 is reset so that the S/N equals 500. Finally, spectra are truncated to delete data at the ends of the orders which cannot be calibrated, using the following wavelength ranges:

order	wavelength range ( $\mu\text{m}$ )
SL2	5.10 – 7.59
SL-bonus	7.73 – 8.39
SL1	7.59 – 14.33
LL2	14.20 – 20.54
LL-bonus	19.28 – 21.23
LL1	20.46 – 37.00

Note that from 20.46 to 20.54  $\mu\text{m}$ , all three LL segments are valid. The regions of overlap between segments are the regions used to determine corrections for discontinuity.

#### 2.1.4 High-resolution spectra

This data delivery also contains spectra observed with the SH and LH modules. In these modules, the nod positions are close together compared to the size of the point-spread function (PSF), forcing us to use dedicated background observations, matching in the number of cycles and integration time, for background subtraction. However, these backgrounds were generally not obtained until about two years into the Spitzer mission. Consequently, for many of these early observations, we must skip the background-subtraction step.

From this point forward, the data processing follows a similar sequence as for SL and LL. Images were cleaned of pixels with NaNs, flagged as rogues, or identified as otherwise flawed using `imclean.pro`. Spectra were extracted using a full-slit extraction, which integrates all of the signal in the slit.

The spectra were calibrated using  $\xi$  Dra (K2 III) as a standard. The assumed “truth” spectrum of  $\xi$  Dra is based on a model by Decin et al. (2004)<sup>1</sup>, but with some modifications. First, the OH band strength was increased by 60% to reflect the strength as observed by the IRS in LL2. Second, the overall photometry was dropped by 3% to match the low-resolution photometric calibration (and the MIPS 24  $\mu\text{m}$  calibration). Finally, we have shifted the shape of the spectrum by 1% from 15.5 to 10  $\mu\text{m}$  so that the SH data agree with the spectra of the same sources in SL. As before, Sloan et al. (2011) are preparing a more thorough explanation of these steps.

As with the low-resolution modules, the final step in the data reduction is to stitch the segments together and trim the extraneous wavelengths. Note that SH was stitched to LH, but no orders were adjusted relative to other orders within the same module, because they were obtained at the same time with identical telescope pointing. The wavelength ranges adopted are as follows:

---

<sup>1</sup><http://irsa.ipac.caltech.edu/data/SPITZER/docs/irs/calibrationfiles/decinmodels/>

	SH wavelength	LH wavelength
order	range ( $\mu\text{m}$ )	range ( $\mu\text{m}$ )
20	9.87–10.40	19.06–19.78
19	10.40–10.96	19.78–20.91
18	10.96–11.60	20.91–22.11
17	11.60–12.32	22.11–23.48
16	12.32–13.12	23.48–25.10
15	13.12–14.08	25.10–26.79
14	14.08–15.09	26.79–28.83
13	15.09–16.32	28.83–31.45
12	16.32–17.77	31.45–34.07
11	17.77–19.47	34.07–36.92

### 2.1.5 Quality control of the data

The Basic Calibrated Data (BCD) generated by the Spitzer pipeline was checked visually by members of the SAGE-Spec team. Various data errors were flagged, and BCDs which would require deviation from the standard processing (Sect. 2.1.2) were noted. Errors found included FUDL (Fast Uplink Downlink) errors, caused by improper data transmission from the spacecraft, cosmic ray hits on the CCD, spectral images which contained more than one spectral trace (i.e., detection of a nearby source in addition to the targeted source) and “jailbarring”, where repeating vertical patterns (residuals) every four columns are left by Spitzer’s A/D converters in cases of a high background on the peak-up arrays (e.g., if the emission from a bright source happens to fall on a peak-up array). In addition, background emission or gradients may have required a change in the standard subtraction algorithm, as detailed above (Sect. 2.1.2). One DCE (Data Collection Event) was visually examined per EXPID (exposure ID), of which there were usually several per module in each BCD. In general, these errors were corrected by:

**FUDL errors:** The spectra from the affected images were dropped from further consideration. In addition, images with FUDL errors were not used for background subtraction.

**cosmic rays:** Most cosmic ray hits were flagged as such and replaced by our `imclean.pro` procedure. Images with unflagged cosmic ray hits were treated in the same way as images with FUDL errors if the affected pixels were in the vicinity of the source (or the source in another image if the affected image was used as a background).

**multiple sources and background issues:** These generally required that we modify the background subtraction scheme. In some cases, we were forced to drop one of the nod spectra from consideration because there was no way to avoid problems caused by other sources or background gradients (either in the target image or in a background image). In a few cases, we were unable to mitigate for the problems, and these are noted in Table B.1.

### 2.1.6 Caveats

Users of the staring-mode IRS spectra should be sure to examine the error bars to the spectra because these they indicate confidence limits and potential problems with the data. In par-

ticular, large error bars throughout a spectral segment indicate that the two spectra from the individual nod positions do not agree, probably due to additional sources or background gradients in the slit which we were unable to correct. Also, a large error bar for a single pixel when surrounded by much smaller error bars indicates that at that wavelength, one of the two nod spectra contained a large spike or divot that was rejected when the nods were combined into a single spectrum. The error bar was calculated based on the rejected datum and retained.

Users should also be aware that the LL slit is significantly larger than the SL slit (10" across compared to 3.6"), and that many of the SAGE-Spec sources show some spatial structure. Often, the SL segments were normalized up to the LL segments more than the ~10–15% expected for random pointing errors for unresolved sources. The CORRSL2, CORRSL1, CORRL2, and CORRL1 keywords in the spectral file headers contain the factors by which each segment was divided to align the spectra; anything smaller than 0.85 indicates a spatially extended source.

The large LL slit often contains excess background emission, which will result in the spectrum beginning to rise in the LL1 spectral segment. This rise to the red is often, but not always, accompanied by larger error bars, since the spectra from the sky subtraction will have differing degrees of success in the two nods in these cases.

### 2.1.7 Point source classification

All IRS spectra of point sources will be classified according to object type and spectral type. In delivery #3 we provide the object classification for the 197 original SAGE-Spec sources, and the remainder will be delivered in 2011. Point sources are classified as follows: low mass ( $M < 8 M_{\odot}$ ) post-Main Sequence stars are classified by chemistry (O- or C-rich) and by evolutionary stage (Asymptotic Giant Branch; post-Asymptotic Giant Branch; and Planetary Nebula), hence our groupings O-AGB, O-PAGB, O-PN, C-AGB, C-PAGB, C-PN. O-PAGB has a subgroup for RV Tauri stars, RVTAU. Red supergiants have a class of their own, RSG. Young stellar objects can be identified as YSO1–YSO3 (increasing in evolution) and YSO4 (candidate Herbig AeBe stars). Stars showing a stellar photosphere, but no additional dust or gas features are classified as STAR. We also distinguish galaxies (GAL), and HII regions (HII). Finally, we use the classification OTHER for objects of *known type* which do not fit into another category (e.g., R Coronae Borealis stars), and also UNK for objects which cannot be classified (unknown objects). For full details of the classification process, please see Woods et al. (2011).

## 2.2 Extended sources

Table 2.1: SAGE-Spec IRS Extended Regions

Name	RA(2000)	Dec(2000)	IRS SL AORID	IRS LL AORID	MIPS-SED AORID
SSDR 1	83.009083	-68.470444	22460928	22460928	22465024
SSDR 2	85.925042	-68.252056	22461184	22461184	22465280
SSDR 3	78.931834	-68.055639	22461440	22461440	22465536
SSDR 4	71.920208	-67.208611	22461696	22461696	22465792

continued on next page...

Table 2.1 – continued from previous page

Name	RA(2000)	Dec(2000)	IRS SL AORID	IRS LL AORID	MIPS-SED AORID
SSDR 5	88.975792	-68.199194	22461952	22461952	22466048
SSDR 6	86.817875	-70.715417	22462208	22462208	22466304
SSDR 7	83.789000	-70.056722	22462464	22462464	22466560
SSDR 8	81.604875	-67.485583	22462720	22462720	22466816
SSDR 9	83.044708	-68.353000	22479360	22479360	22480384
SSDR 10	83.095625	-66.478194	22479872	22479872	22480896
SSDR 11	85.915208	-68.771833	24241664	24241664	24242432
SSDR 12	82.779583	-68.320000	24242176	24242176	—
DEM L 8	73.026292	-66.924194	22469120	22469120	22474240
DEM L 10	73.049584	-69.345306	22469376	22469376	22474496
DEM L 34	74.208709	-66.413889	22469632	22469632	22474752
DEM L 40	74.421709	-67.648306	22469888	22469888	22475008
DEM L 55	75.421708	-70.646889	22470144	22470144	22475264
DEM L 86	77.483292	-68.900889	22470400	22470400	22475520
DEM L 188	81.267917	-71.463111	22470656	22470656	22475776
DEM L 243	83.879583	-66.044111	22470912	22470912	22476032
DEM L 308	86.224583	-67.348389	22471168	22471168	22476288
DEM L 323	87.218292	-70.064305	22471424	22471424	22476544
30 Dor	84.7063	-69.0993	18630144	18635008	18633728

### 2.2.1 Observation settings

All the IRS extended source observations in this data delivery were obtained using the standard IRS spectral mapping template. The names, central coordinates, and AOR numbers for the IRS observations are given in Table 2.1. The regions mapped were chosen to be large enough to sample the entire region or a representative region (usually a radial strip). All the observations were paired with dedicated background observations taken in a low surface brightness region located outside of the LMC.

### 2.2.2 Data processing

The pipeline-reduced IRS spectral mapping data were retrieved from the Spitzer archive (versions S17.0.4 to S18.7.0). These individual observations were combined into spectral cubes using the CUBISM software (Smith et al. 2007). The dedicated off-LMC background observations were subtracted from the on- and off-source mosaics prior to combining using CUBISM. Each extended source spectral mapping observation results in six different order cubes (except for 30 Dor that only has four order cubes). These six different order cubes per object are the deliverables for this release. Later releases will include a single merged spectral cube covering the entire IRS spectral range. Full astrometry for each cube (both spatial and spectral) is captured as part of the FITS header of the spectral cube.

### 2.2.3 Quality control of the data

The quality control on the IRS spectral mapping observations was focused on examining the mosaics. Extracted IRS spectra frequently show offsets between orders and modules, with a variety of causes. Most common for extended sources are differences in what part of the sky is sampled by different size slits and a wavelength-dependent telescope beam that is larger than the slit. As described in the IRS Instrument Handbook (Chapter 4), the spectra are calibrated for unresolved point sources. Not all of the light from such a source is present in such a spectrum – some does not fall down the slit (Slit Loss), and some does not fall in the standard extraction aperture (Aperture Loss). For a source with uniform surface brightness on spatial scales larger than the slit and the telescope beam, light lost from the part of the sky being measured is compensated by light from neighboring parts of the sky that get spread into the Slit and Aperture by the finite spatial response (point spread function or beam). The extracted spectrum of such a uniform source must be divided by the Slit and Aperture Loss Correction Factors, effectively undoing the corrections required for a point source. In reality, extended sources are neither unresolved point sources nor have uniform surface brightness, so the precise correction to use is unknown. We adopt standard practice for IRS extended source software such as CUBISM, and remove the Slit and Aperture Loss Correction Factors (i.e., we use the uniform-source calibration). Point or nearly point sources in the map will have lower flux densities than they should, and the discrepancy will vary by module. Cubes created with both the uniform-source and point-source calibrations still have offsets between orders and modules, especially for fainter regions.

Many investigators calculate and apply a multiplicative correction between IRS modules, to “order-match” the spectra. We found that for faint sources, a purely multiplicative correction could not universally match all orders, modules, and simultaneously IRAC and MIPS photometry, but that an additive offset is sometimes present, which we believe to be largely due to incorrect dark current subtraction in the SSC pipeline.

The dark current has been observed to vary with time and chip location. This is described as “dark settle” in the IRS Data Reduction Handbook (v4.0.1, Recipe 11). That recipe, and SSC-provided software for correcting dark settle, applies to the LH module, but our analysis and private communication with SSC suggests that the issue likely exists for all modules. If the dark frame used in the BCD pipeline is different from the actual dark current, an additive offset as a function of chip location (hence wavelength and spatial position) will be introduced. More generally, since the SSC has adopted average darks for the entire mission, variations in the dark during the mission, and any errors in modelling the time-dependent zodiacal light, will also result in additive errors in extracted spectra. The SSC-provided dark-settle correction software calculates the dark current as a function of detector row from the pixels between spectral orders. We have modified their software to operate on the SL and LL modules, but SL in particular is challenging to correct because there is very little inter-order area on the chip. The regions between the spectral data and the peak-up imagers (PUI) are often contaminated by stray light from bright sources in the PUI. See Section 5.1.16 of the IRS Instrument Handbook (v4.0) for a description of stray light and a figure showing the layout of the spectral orders and PUI on the detector.

Our dark-settle correction code operates on the BCD data with the following steps:

1. subtract the median off-source background frame associated with the AOR (the intent is to correct differences in the dark current between the on-source and off-source observations, which is a smaller effect than the total dark current)
2. divide by the flat-field
3. mask all active parts of the chip (spectral on-order, PUI, and a few small manually determined very bad groups of pixels)
4. calculate the resistant mean of the unmasked pixels in each row, yielding a 1-dimensional correction as a function of row
5. smooth the correction with a Savitzky-Golay smoothing filter (Savitsky & Golay 1964), requiring that the correction be small at the top and bottom of the chip
6. subtract the correction from each row of the 2-dimensional data
7. re-multiply by the flat-field

Subsequent to the dark-settle correction, spectral cubes are re-created from this corrected BCD data using CUBISM.

We find that for most of the IRS mapping data in the SAGE-Spec program, applying the darksettle correction to the BCD frames improves matching between orders and modules in spectra extracted from subsequently reconstructed spectral cubes. However, some of the faintest maps do not show significant improvement, and some data show a larger number of hot/dark pixels than in the uncorrected cubes. The latter problem arises because the dark-settle operation applies a background (off-source) subtraction, which tends to make rogue pixels deviate by less relative to the data's rms, and therefore are harder for CUBISM's outlier detector algorithm to find and flag. Due to the uncertainties, we have decided not to deliver the dark-settle corrected cubes, but are happy to work with investigators who wish to use them, to determine if they improve a particular scientific inquiry. Please contact Remy Indebetouw directly ([remy@virginia.edu](mailto:remy@virginia.edu)).

## Chapter 3

# MIPS-SED spectroscopy

### 3.1 Point sources

#### 3.1.1 Observation settings

All the MIPS-SED point source observations in this data delivery were obtained using the standard MIPS-SED point source template. The chop distance and total exposure time was adjusted based on the nearby sources seen in the MIPS 70  $\mu\text{m}$  image and the measured MIPS 70  $\mu\text{m}$  photometry, respectively.

#### 3.1.2 Data processing

The MIPS-SED data were processed through the MIPS Data Analysis Tool (DAT, v3.10, 3 Jul 2007). The details of the MIPS DAT are given by Gordon et al. (2005). The product of the MIPS DAT is both on-source background subtracted (on-off), on-source only, and off-source only rectified mosaics combining all the appropriate observations in an AOR. For the majority of the sources, the on-source background subtracted mosaics (on-off) was used as this removes the majority of the background emission and residual instrumental signatures.

The spectra were extracted from the 2D rectified mosaics. First, a spatial profile was created by collapsing the 2D mosaic along the wavelength axis. In most cases, the maximum in the spatial profile identified the source position along the slit. The extraction was done using the standard width of 5 pixels with residual background subtraction done using two regions 3 pixels wide located on either side of the source. In the few cases where the off-source chop position was contaminated by another source, the on-source data was used and the background subtraction using the two background regions on either side of the source. For a few, faint sources, the source position was fixed to the default location.

The extracted spectra were trimmed to reject all data beyond 95 microns as these wavelengths are contaminated by 2nd order flux. The spectra were corrected to infinite aperture and calibrated using the results given by Lu et al. (2008).



### 3.1.3 Quality control of the data

The quality control on the MIPS-SED observations was focused on examining the mosaics and spatial profile of the source. The quality of a spectrum was deemed as “good” if there was no source in the off-source position and the spatial profile was distinctly a point source. A source was “ok” if there was a faint source in the off-source position or if its spatial profile was not as simple as a single point source, but still enough like a point source to get a decent extraction. A source was “poor” if there was a bright source in the off-source mosaic or it was very extended. A source was “bad” if there was no reasonable source to be extracted.

## 3.2 Extended sources

### 3.2.1 Observation settings

All the MIPS-SED extended source observations in this data delivery were obtained using the standard MIPS-SED mapping template. The names, central coordinates, and AOR numbers for the MIPS-SED observations are given in Table 2.1. The regions mapped were chosen to be large enough to sample the entire region or a representative region (usually a radial strip). All the observations were paired with dedicated background observations taken in a low surface brightness region located outside of the LMC.

### 3.2.2 Data processing

The MIPS-SED data were processed through the MIPS Data Analysis Tool (DAT, v3.10, 3 Jul 2007). The details of the MIPS DAT are given by Gordon et al. (2005). The product of the MIPS DAT is both on-source background subtracted (on-off), on-source only, and off-source only rectified mosaics combining all the appropriate observations in an AOR.

For each spectral map, spectral cubes were created using custom IDL code (C. Engelbracht et al., in prep.) that uses the on-source and off-source MIPS DAT products to create a 3D spectral cube (which is basically an image at each wavelength). The dedicated off-LMC background observations were subtracted from the on- and off-source mosaics prior to combining using the custom IDL software. Full astrometry for the cube (both spatial and spectral) is captured as part of the FITS header of the spectral cube. The extended source calibration of this code has been checked between similar MIPS SED mapping and  $70\ \mu\text{m}$  imaging observations in the SINGS Legacy sample (C. Engelbracht et al., in prep.).

The spectral cubes include data beyond 95 microns, but this data should be used with extreme caution as these wavelengths are contaminated by 2nd order flux.

### 3.2.3 Quality control of the data

The quality control on the MIPS-SED spectral mapping observations was focused on examining the mosaics and fitted continuum/line strengths. Reasonable results were obtained. An additional check was made between extracted spectra of the entire regions and the equivalent

### 3.2. EXTENDED SOURCES    CHAPTER 3. MIPS-SED SPECTROSCOPY

70  $\mu\text{m}$  photometry of the same regions. The results of this additional check indicates that the flux calibration of the MIPS-SED spectral mapping is as expected.

# Appendix

## Appendix A

# Availability of spectra and photometry

Table A.1: Photometry and spectroscopy for SAGE-Spec sources observed in IRS staring mode.<sup>1</sup>

SAGE-Spec source ID	UBVI	JHK	IRAC	MIPS	SL	LL	MIPS-SED
1	BVI	✓	✓	24	✓	—	—
2	—	✓	✓	24, 70	✓	✓	✓
3	✓	✓	✓	24	✓	✓	—
4	✓	✓	✓	24	✓	✓	—
5	BVI	✓	✓	24, 70	✓	✓	—
6	✓	✓	✓	24	✓	✓	—
7	BVI	✓	✓	24	✓	✓	—
8	BVI	✓	✓	24	✓	✓	—
9	—	—	✓	24	✓	✓	—
10	BVI	✓	✓	24, 70	✓	✓	—
11	✓	✓	✓	✓	✓	✓	—
12	BVI	✓	✓	24	✓	—	—
13	✓	✓	✓	24	✓	—	—
14	UBV	✓	✓	✓	✓	✓	—
15	—	✓	✓	24	✓	—	—
16	UBV	✓	✓	70	✓	—	—
17	—	—	—	24	—	✓	✓
18	—	—	✓	24	✓	✓	—
19	—	✓	✓	24	✓	—	—
20	✓	✓	✓	24, 160	✓	✓	—
21	✓	✓	✓	24	✓	✓	—
22	✓	✓	✓	24	✓	✓	—
23	✓	✓	✓	24	✓	—	—
24	—	—	—	—	✓	—	—

continued on next page...

APPENDIX A. AVAILABILITY OF SPECTRA AND PHOTOMETRY

Table A.1 – continued from previous page

SAGE-Spec source ID	UBVI	JHK	IRAC	MIPS	SL	LL	MIPS-SED
25	✓	✓	✓	24, 70	✓	✓	—
26	✓	✓	✓	24	✓	✓	—
27	✓	✓	✓	24	✓	✓	—
28	✓	✓	✓	24	✓	✓	—
29	✓	✓	✓	24	✓	✓	—
30	✓	✓	✓	24	✓	—	—
31	✓	✓	✓	24	✓	—	—
32	✓	✓	✓	24	✓	—	—
33	✓	✓	✓	24	✓	—	—
34	✓	✓	✓	✓	✓	✓	—
35	✓	✓	✓	24	✓	—	—
36	✓	✓	✓	24	✓	—	—
37	✓	✓	✓	24	✓	—	—
38	✓	✓	✓	24	✓	✓	—
39	✓	✓	✓	24	✓	✓	—
40	✓	✓	✓	✓	✓	✓	—
41	UBV	✓	✓	24	✓	—	—
42	✓	✓	✓	24	✓	✓	—
43	✓	✓	✓	24	✓	—	—
44	BVI	✓	✓	24, 70	✓	✓	—
45	—	✓	✓	24	✓	—	—
46	—	✓	✓	24	✓	—	—
47	—	✓	✓	24	✓	—	—
48	—	✓	✓	24	✓	—	—
49	—	✓	✓	24	✓	—	—
50	✓	✓	✓	24	✓	✓	—
51	—	✓	✓	24	✓	✓	—
52	—	✓	✓	24, 70	✓	✓	—
53	BV	✓	✓	24, 70	✓	✓	—
54	BVI	✓	✓	24	✓	✓	—
55	BVI	✓	✓	24	✓	✓	—
56	✓	✓	✓	24	✓	✓	—
57	✓	✓	✓	24	✓	—	—
58	✓	✓	✓	24	✓	—	—
59	BV	✓	4.5, 5.8, 8.0	24	✓	—	—
60	✓	✓	✓	24	✓	✓	—
61	✓	✓	✓	24	✓	✓	—
62	✓	✓	✓	24, 70	✓	✓	—
63	BVI	✓	✓	24	✓	—	—

continued on next page...

APPENDIX A. AVAILABILITY OF SPECTRA AND PHOTOMETRY

Table A.1 – continued from previous page

SAGE-Spec source ID	UBVI	JHK	IRAC	MIPS	SL	LL	MIPS-SED
64	✓	✓	✓	24	✓	✓	—
65	—	✓	✓	24	✓	✓	—
66	BVI	✓	✓	24	✓	✓	—
67	✓	✓	✓	24	✓	—	—
68	UBV	✓	✓	24	✓	—	—
69	✓	✓	✓	24, 70	✓	✓	—
70	—	K	4.5, 5.8, 8.0	24	✓	✓	—
71	—	✓	✓	24	✓	✓	—
72	✓	✓	✓	24	✓	—	—
73	✓	✓	✓	24	✓	✓	—
74	✓	✓	✓	24, 70	✓	✓	—
75	✓	✓	✓	24	✓	✓	—
76	✓	✓	✓	24	✓	—	—
77	✓	✓	✓	24	✓	—	—
78	BVI	✓	✓	✓	✓	✓	—
79	BVI	✓	✓	24	✓	—	—
80	✓	✓	✓	24	✓	✓	—
81	✓	✓	✓	24	✓	—	—
82	✓	✓	✓	24	✓	✓	—
83	BVI	✓	✓	24	✓	—	—
84	✓	✓	✓	24, 70	✓	✓	—
85	✓	✓	✓	24	✓	✓	—
86	✓	✓	✓	24	✓	—	—
87	—	✓	✓	24	✓	—	—
88	✓	✓	✓	—	✓	—	—
89	✓	✓	✓	24	✓	—	—
90	✓	✓	✓	24	✓	✓	—
91	—	✓	✓	24	✓	—	—
92	✓	✓	✓	24, 70	✓	✓	—
93	✓	✓	✓	24	✓	✓	—
94	✓	✓	✓	24	✓	✓	—
95	✓	✓	✓	24	✓	✓	—
96	✓	✓	✓	24	✓	✓	—
97	✓	✓	✓	✓	✓	✓	✓
98	BVI	✓	✓	24	✓	✓	—
99	BVI	✓	✓	24	✓	—	—
100	✓	✓	✓	24	✓	✓	—
101	BV	✓	✓	✓	✓	✓	—
102	—	✓	✓	24, 70	✓	✓	✓

continued on next page...

APPENDIX A. AVAILABILITY OF SPECTRA AND PHOTOMETRY

Table A.1 – continued from previous page

SAGE-Spec source ID	UBVI	JHK	IRAC	MIPS	SL	LL	MIPS-SED
103	—	✓	✓	24	✓	✓	—
104	UBV	✓	✓	✓	✓	✓	—
105	BVI	✓	✓	24	✓	✓	—
106	✓	✓	✓	24, 70	✓	✓	—
107	✓	✓	✓	24	✓	✓	—
108	✓	✓	✓	✓	✓	✓	—
109	✓	✓	✓	24, 70	✓	✓	—
110	✓	✓	✓	24	✓	—	—
111	✓	✓	✓	24	✓	✓	—
112	UBV	—	✓	24	✓	—	—
113	✓	✓	✓	24	✓	✓	—
114	✓	✓	✓	24, 70	✓	✓	✓
115	✓	✓	✓	24	✓	—	—
116	✓	✓	✓	24	✓	✓	—
117	UBI	✓	✓	24	✓	✓	—
118	✓	✓	✓	24	✓	✓	—
119	✓	✓	✓	24	✓	✓	—
120	✓	✓	✓	24	✓	—	—
121	✓	✓	✓	24, 70	✓	✓	—
122	UB	✓	✓	24	✓	✓	—
123	UB	✓	✓	24	✓	✓	—
124	✓	✓	✓	24	✓	—	—
125	—	✓	✓	24, 70	✓	✓	—
126	✓	✓	✓	24	✓	✓	—
127	✓	✓	✓	24	✓	—	—
128	UBV	✓	✓	24	✓	✓	—
129	UBV	✓	✓	24	✓	✓	—
130	BVI	✓	✓	24	✓	✓	—
131	✓	✓	✓	24	✓	✓	—
132	—	✓	✓	24	✓	—	—
133	BVI	✓	✓	24	✓	—	—
134	UBV	✓	✓	24	✓	—	—
135	BV	✓	✓	24	✓	✓	—
136	—	✓	✓	24	✓	—	—
137	✓	✓	✓	24	✓	✓	—
138	✓	✓	✓	24, 70	✓	✓	—
139	✓	✓	✓	24	✓	—	—
140	BV	✓	✓	24	✓	✓	—
141	✓	✓	✓	24	✓	✓	—

continued on next page...

APPENDIX A. AVAILABILITY OF SPECTRA AND PHOTOMETRY

Table A.1 – continued from previous page

SAGE-Spec source ID	UBVI	JHK	IRAC	MIPS	SL	LL	MIPS-SED
142	✓	✓	✓	24	✓	—	—
143	✓	✓	✓	24	✓	—	—
144	✓	✓	✓	24, 70	✓	✓	—
145	BVI	✓	✓	24	✓	✓	—
146	✓	✓	✓	24	✓	✓	—
147	UBV	✓	✓	24	✓	✓	—
148	✓	✓	✓	24	✓	—	—
149	✓	✓	✓	24	✓	✓	—
150	✓	✓	✓	24, 70	✓	✓	—
151	✓	✓	✓	24	✓	✓	—
152	✓	✓	✓	24	✓	—	—
153	✓	✓	✓	24	✓	—	—
154	✓	✓	✓	24, 70	✓	✓	—
155	BVI	✓	✓	24	✓	—	—
156	BVI	✓	✓	24	✓	✓	—
157	✓	✓	✓	24	✓	✓	—
158	BV	✓	✓	24	✓	✓	—
159	✓	✓	✓	24	✓	—	—
160	✓	✓	✓	24	✓	✓	—
161	✓	✓	✓	24	✓	—	—
162	✓	✓	✓	24	✓	✓	—
163	✓	✓	✓	24, 70	✓	✓	✓
164	BVI	HK	✓	24, 70	✓	✓	—
165	✓	✓	✓	24	✓	✓	—
166	✓	✓	✓	24	✓	✓	—
167	—	—	✓	24	✓	✓	—
168	UBV	✓	✓	24, 70	✓	✓	—
169	UBV	✓	✓	24	✓	✓	—
170	UBV	✓	✓	24	✓	✓	—
171	UBV	✓	✓	24	✓	✓	—
172	✓	✓	✓	24	✓	✓	—
173	✓	✓	✓	24	✓	—	—
174	✓	✓	✓	24	✓	✓	—
175	✓	✓	✓	24	✓	✓	—
176	BVI	✓	✓	24	✓	—	—
177	✓	✓	✓	24	✓	✓	—
178	✓	✓	✓	24	✓	—	—
179	BVI	✓	✓	24	✓	—	—
180	✓	✓	✓	24	✓	✓	—

continued on next page...



APPENDIX A. AVAILABILITY OF SPECTRA AND PHOTOMETRY

Table A.1 – continued from previous page

SAGE-Spec source ID	UBVI	JHK	IRAC	MIPS	SL	LL	MIPS-SED
181	✓	✓	✓	24	✓	✓	—
182	✓	✓	✓	24	✓	✓	—
183	✓	✓	✓	24, 70	✓	✓	—
184	BVI	✓	✓	24, 70	✓	✓	—
185	—	✓	✓	24	✓	✓	—
186	✓	✓	✓	24	✓	✓	—
187	✓	✓	✓	24	✓	✓	—
188	✓	✓	✓	24	✓	—	—
189	BVI	✓	✓	24	✓	—	—
190	BVI	—	✓	24, 70	✓	✓	—
191	✓	✓	✓	24	✓	—	—
192	✓	✓	✓	24	✓	✓	—
193	✓	✓	✓	24	✓	✓	—
194	BVI	✓	✓	24	✓	—	—
195	—	✓	✓	24	✓	—	—
196	✓	✓	✓	24, 70	✓	✓	—
197	✓	✓	✓	24	✓	—	—

Table A.1: <sup>1</sup>Photometry for SSID17, 24, 125 and 133 has been altered since delivery #1. The present table represents the best available photometry.

## Appendix B

# Quality control results for SAGE-Spec IRS spectra

Table B.1: Data processing summary (see key below table).

ID	Reduction method	SL	LL	Notes
1	default	—	—	
2	default	—	—	
3	default	—	—	
4	default	J-Wa	—	
5	default	—	—	
6	modified	Ray-Mc-Notes	B-Wa	SL – 0300: Ray
7	default	—	N-Wa	
8	default	—	—	
9	default	—	—	
10	modified	—	S-Mc-1Dx,2Da	
11	default	—	—	
12	default	J-Wa	—	
13	modified	B-Mc-Dn	—	
14	default	—	—	
15	default	J-Wa	—	
16	default	—	—	
17	modified	—	—	
18	default	—	—	
19	default	J-Wa	—	
20	modified	X-Mc-Notes	—	SL – 0200: FUDL, 0400: Dx
21	default	—	—	
22	modified	P-Mc-2Dn	S-Wa	
23	default	—	—	
24	modified	F-Mi-Dn	—	
25	modified	B-Mc-Dn	B-Mc-C2	
26	default	J-Wa	—	
27	default	S-Wa	—	

continued on next page...

APPENDIX B. QUALITY CONTROL RESULTS FOR IRS SPECTRA

Table B.1 – continued from previous page

ID	Reduction method	SL	LL	Notes
28	default	S-Wa	S-Wa	
29	default	J-Wa	—	
30	default	J-Wa	—	
31	default	J-Wa	—	
32	default	—	—	
33	default	J-Wa	—	
34	modified	B,X-Mc-Notes	—	SL – 0400: bad pixel block
35	default	—	—	
36	default	—	—	
37	default	—	—	
38	modified	J,Ray-Wa-Notes	—	SL – 0502: Ray
39	modified	—	S-Mc-Da	
40	default	—	—	
41	default	—	—	
42	default	—	—	
43	default	—	—	
44	modified	B-Wa	S-Mc-1Da	
45	default	J-Wa	—	
46	default	—	—	
47	default	—	—	
48	default	J-Wa	—	
49	modified	B-Mc-Dn	—	
50	modified	B-Mc-Dn,Notes	B-Mc-Da	SL – 14.2 $\mu$ m spike
51	modified	—	S-Mc-1C1	
52	default	—	—	
53	default	—	—	
54	default	J-Wa	—	
55	modified	—	N-Mc-1Da	
56	modified	B-Mc-1Dn	S-Wa	
57	default	—	—	
58	modified	X-Mc-Notes	—	SL – 0404: bad pixel block
59	default	S-Wa	—	
60	modified	—	N-Mc-1Da	
61	default	—	S-Wa	
62	default	—	—	
63	default	—	—	
64	default	—	—	
65	modified	—	S-Mc-1C1	
66	default	—	B-Mc-1Da1,1Dx2	
67	default	—	—	
68	default	—	—	
69	modified	B-Mi-Dn	B-Mi-1Da	
70	default	E-Wa	—	
71	modified	—	N-Mi-Da	
72	modified	S-Mc-Dn	—	
73	default	—	B-Wa	

continued on next page...

APPENDIX B. QUALITY CONTROL RESULTS FOR IRS SPECTRA

Table B.1 – continued from previous page

ID	Reduction method	SL	LL	Notes
74	default	—	—	
75	default	—	S-Wa	
76	default	—		
77	default	—		
78	default	J-Wa	—	
79	default	—		
80	modified	—	S-Mc-C1	
81	default	—		
82	default	—	—	
83	default	N-Wa		
84	default	—	—	
85	modified	J-Wa	S-Mc-1Cn1	
86	default	—		
87	modified	B,J-Mi-1Dn		
88	modified	B,S-Mi-Dn		
89	default	S-Wa		
90	default	—	—	
91	modified	B-Mc-2Dn		
92	modified	X-Mc-Notes	—	SL – 0402: FUDL, 0202: Dx, 0302: Ray
93	modified	—	B,S-Mc-Da	
94	default	—	—	
95	modified	B-Mc-1Dn	B-Mc-1Da	
96	default	—	—	
97	default	—	—	
98	modified	—	S-Mc-Notes	LL – 0802: FUDL, 0902: Da
99	default	—		
100	default	—	N-Wa	
101	default	—	—	
102	default	—	—	
103	modified	—	S-Mc-1Da	
104	modified	J,Ray-Mc-Notes	—	SL – 0502: Ray
105	modified	J-Wa	B-Mi-1Dx,2Da	
106	modified	—	B-Mc-1C1	
107	default	—	—	
108	modified	B-Mi-Dn	S-Mc-Da	
109	modified	—	S-Mc-1Cn2	
110	default	—		
111	default	—	—	
112	default	—		
113	modified	—	S-Mc-1Da	
114	default	J-Wa	N-Wa	
115	default	—		
116	modified	J,S-Mc-Notes	S-Mc-2Da	SL – 0401: Ray, 0202: FUDL, 0402: Dx
117	modified	S-Mc-Notes	N,S-Fa	SL – Ridge constrained
118	default	—	—	
119	modified	—	S-Mi-Da	

continued on next page...

APPENDIX B. QUALITY CONTROL RESULTS FOR IRS SPECTRA

Table B.1 – continued from previous page

ID	Reduction method	SL	LL	Notes
120	default	—		
121	default	—	—	
122	default	—	S-Wa	
123	modified	—	B-Mc-1Da	
124	default	—		
125	default	—	—	
126	default	—	—	
127	default	S-Wa		
128	modified	—	S-Mc-Da	
129	default	—	—	
130	default	—	—	
131	modified	J-Wa	B-Mc-Da	
132	default	—		
133	default	—		
134	default	—		
135	default	—	—	
136	default	—		
137	default	—	B-Wa	
138	default	—	—	
139	default	B-Wa		
140	default	—	—	
141	default	J-Wa	B,S-Wa	
142	default	—		
143	default	—		
144	default	—	—	
145	default	—	B,S-Wa	
146	default	—	N-Wa	
147	default	—	—	
148	modified	B-Mc-1Dn		
149	default	—	N-Wa	
150	default	—	—	
151	default	—	—	
152	default	B-Wa		
153	default	—		
154	default	—	—	
155	default	—		
156	modified	B,S-Mc-Dn	B,S,N-Wa	
157	default	—	—	
158	modified	S-Mc-2Dn	S-Wa	
159	default	—		
160	modified	B,J-Mc-Dn	N-Fa	
161	modified	J,P-Mi-Dn		
162	modified	N-Wa	S-Mc-1Da	
163	default	—	S-Wa	
164	modified	B,J-Mi-1Dn	—	
165	modified	Ray-Wa	S-Mi-Da	

continued on next page...

APPENDIX B. QUALITY CONTROL RESULTS FOR IRS SPECTRA

Table B.1 – continued from previous page

ID	Reduction method	SL	LL	Notes
166	default	—	—	
167	modified	—	B-Mc-1Cn1	
168	default	—	—	
169	modified	B-Mc-1Dn	B-Mi-Cn2	
170	modified	—	S-Mi-1Da	
171	modified	S-Mc-Notes	S-Mi-Notes	SL – 0401: FUDL, 0201: Dx LL – 1Da, 2Dn1, 2Dx2
172	modified	—	S-Mc-Da	
173	modified	B-Mc-1Dn		
174	modified	F-Mi-Dn	F-Wa	
175	modified	X-Mc-Notes	—	SL – 0301: Ray, not dropped, 0501: Dx
176	default	—	—	
177	default	—	—	
178	default	—	—	
179	modified	B-Mc-1Dn		
180	default	—	N-Wa	
181	default	—	—	
182	default	—	B,N-Wa	
183	default	—	—	
184	modified	—	N-Mc-1Da	
185	default	—	—	
186	default	J-Wa	—	
187	default	—	—	
188	default	—	—	
189	default	—	—	
190	default	—	—	
191	modified	B-Mi-Dn	—	
192	default	—	—	
193	default	—	—	
194	default	—	—	
195	default	—	—	
196	default	—	—	
197	default	—	—	

APPENDIX B. QUALITY CONTROL RESULTS FOR IRS SPECTRA

---

	KEY: –
<b>Reduction method</b>	<i>default</i> – as described in Sect. 2.1.2; <i>modified</i> – the default method of background subtraction, extraction and coadding of spectra was changed in some way, as detailed in a three-part code, constructed as: <problem>-<severity>-<solution>
<b>Problem</b>	<i>J</i> – jailbars in the data. <i>N</i> – significant difference in appearance between two nods. <i>FUDL</i> – FUDL (data download) error. <i>Ray</i> – cosmic ray strike. <i>P</i> – peak-up related problem. <i>B</i> – background issue. <i>S</i> – additional source. <i>E</i> – excess emission. <i>F</i> – very faint source. <i>M</i> – no source. <i>X</i> – other issue.
<b>Severity</b>	<i>Wa</i> – defective data, however no repair was attempted because defect was deemed minor, i.e., did not affect the extraction. <i>Mc</i> – reduction procedure was modified and successfully corrected issue. <i>Mi</i> – reduction procedure was modified and improved the issue but could not fully correct it.
<b>Solution</b>	<i>Fa</i> – there was an issue with the data which could not be improved upon. <i>#Da#</i> – aperture difference (rather than nod difference). Where numbers are included in the code, the first number is the order number, and the second the nod, e.g., 1Da2 is LL1, nod 2 <i>#Dn#</i> – nod difference (rather than aperture difference). <i>#Dx#</i> – cross difference. <i>#C#</i> – co-add was changed (usually by using only one nod).

# Bibliography

- Davies, R. D., Elliott, K. H., & Meaburn, J. 1976, *Memoirs of the Royal Astronomical Society*, 81, 89
- Decin, L., Morris, P. W., Appleton, P. N., Charmandaris, V., Armus, L., & Houck, J. R. 2004, *ApJS*, 154, 408
- Engelbracht, C. W., et al. 2007, *PASP*, 119, 994
- Engelke, C. W. 1992, *AJ*, 104, 1248
- Gordon, K. D., et al. 2005, *PASP*, 117, 503
- Kato, D., et al. 2007, *PASJ*, 59, 615
- Kemper, F., et al. 2010, *PASP*, 122, 683
- Lu, N., et al. 2008, *PASP*, 120, 328
- Meixner, M., et al. 2006, *AJ*, 132, 2268
- Rieke, G. H., et al. 2008, *AJ*, 135, 2245
- Savitsky, A. & Golay, M. J. E. 1964, *Analytical Chem.*, 36, 1627
- Skrutskie, M. F., et al. 2006, *AJ*, 131, 1163
- Smith, J. D. T., et al. 2007, *PASP*, 119, 1133
- van Loon, J. T., et al. 2010, *AJ*, 139, 68
- Woods, P. M., et al. 2011, *MNRAS*, 411, 1597
- Zaritsky, D., Harris, J., Thompson, I. B., & Grebel, E. K. 2004, *AJ*, 128, 1606